Novel Block Ionomers. III. Mechanical and Rheological Properties

Zheng Fang, Shanfeng Wang, Shi Quing Wang, Joseph P. Kennedy

Department of Polymer Science, University of Akron, Akron, Ohio 44325

Received 6 May 2002; accepted 11 June 2002

ABSTRACT: Select rheological (dynamic viscoelastic) and mechanical properties of novel block cationomers and anionomers and their blends have been investigated. The block ionomers were linear di- and triblocks, and symmetric three-arm stars comprising hydrophobic polyisobutylene (PIB) blocks attached to ionized poly(methacrylic acid) ($PMAA^-X^+$, where $X^+ = Na^+, Zn^{2+}$) and poly[2-(dimethylamino)ethyl methacrylate] ($PDMAEMA^+I^-$) blocks. The specific structures investigated were the well-defined diblocks PIB-*b*-$PMAA^-$ and PIB-*b*-$PDMAEMA^+$ and their blends, the triblocks $PMAA^-$-*b*-PIB-*b*-$PMAA^-$ and $PDMAEMA^+$-*b*-PIB-*b*-$PDMAEMA^+$ and their blends, and the three-arm star anionomer $\Phi(\text{PIB-}b\text{-PMAA}^-)_3$. For comparison, the properties of the precursor PIBs and unionized blocks have also been studied. Hydrogen bonding between the carboxyl groups of the PMAA blocks in PIB-*b*-PMAA diblocks leads to inverse micelles. Neutralization of the PMAA by $Zn(AcO)_2$ and quaternization of the PDMAEMA segments by CH_3I in the triblock copolymers and star copolymers yielded ionic domains, which self-assemble and produce physical networks held together by coulumbic interaction. The physical/chemical characteristics of the domains control the viscoelastic behavior and mechanical properties of these block ionomers. The mechanical properties of the various block ionomers were significantly enhanced relative to the precursors, and they were thermally stable below the transition temperature. Further, the thermomechanical properties of these novel materials were satisfactory even above 200°C. © 2003 Wiley Periodicals, Inc. J Appl Polym Sci 88: 1516–1525, 2003

Key words: ionomers; block polymers; blends

INTRODUCTION

Block and star copolymers, particularly those containing both hydrophobic and hydrophilic segments, are of great commercial and scientific interests.[1,2] Mechanical and rheological investigation of block and star polymers provide valuable information in regard to their morphology and microstructure.[3,4]

Eisenberg et al.[5–7] investigated the morphology and structure of poly(styrene-*b*-sodium methacrylate) diblock ionomers in the melt and solution by dynamic mechanical analysis (DMA), transmission electron microscopy (TEM), and small-angle X-ray scattering (SAXS) and found that this system can form very stable reverse micelles.[8] Weiss et al.[9] prepared sulfonated poly(styrene–ethylene/butylene–styrene) triblocks and studied their viscoelastic and mechanical properties. They presented evidence for an ionic network within the styrene-rich phase. Sulfonation substantially improved high-temperature tensile stress and elongation.[9] Storey and Baugh[10] found that even partial (5–20 mol %) sulfonation of the polystyrene blocks of poly(styrene-*b*-isobutylene-*b*-styrene) and similar three-arm star blocks significantly increased the modulus and tensile strength of these materials. Vlassopoulos et al.[11,12] studied the dynamics of linear ω-zwitterionic and mono-, di-, and tri-ω-zwitterionic three-arm star 1,4-polybutadienes and correlated their self-assembly with viscoelastic properties.

In a series of two earlier articles, we described the synthesis and characterization of novel polyisobutylene (PIB)-based diblock, triblock, and three-arm star block anionomers[13] and cationomers.[14] Scheme 1 visualizes the nanoarchitecture of these block ionomers. This article concerns select viscoelastic and mechanical properties of these block and star ionomers and select cationomer/anionomer blends. Significantly, intermolecular self-assembly by hydrogen bonding and ionic aggregation control the viscoelastic and mechanical behavior of these novel materials.

EXPERIMENTAL

The symbols for the block ionomers show the abbreviation for the block followed by a number in parentheses that indicates the degree of polymerization (DP) of the blocks. For example, PMAA(7)-*b*-PIB(160)-

---

Correspondence to: J. P. Kennedy (kennedy@polymer.vakron.edu).

Contract grant sponsor: the National Science Foundation; contract grant number: DMR-99-88808, DMR-0243314, and NSF-0196033.

Journal of Applied Polymer Science, Vol. 88, 1516–1525 (2003)

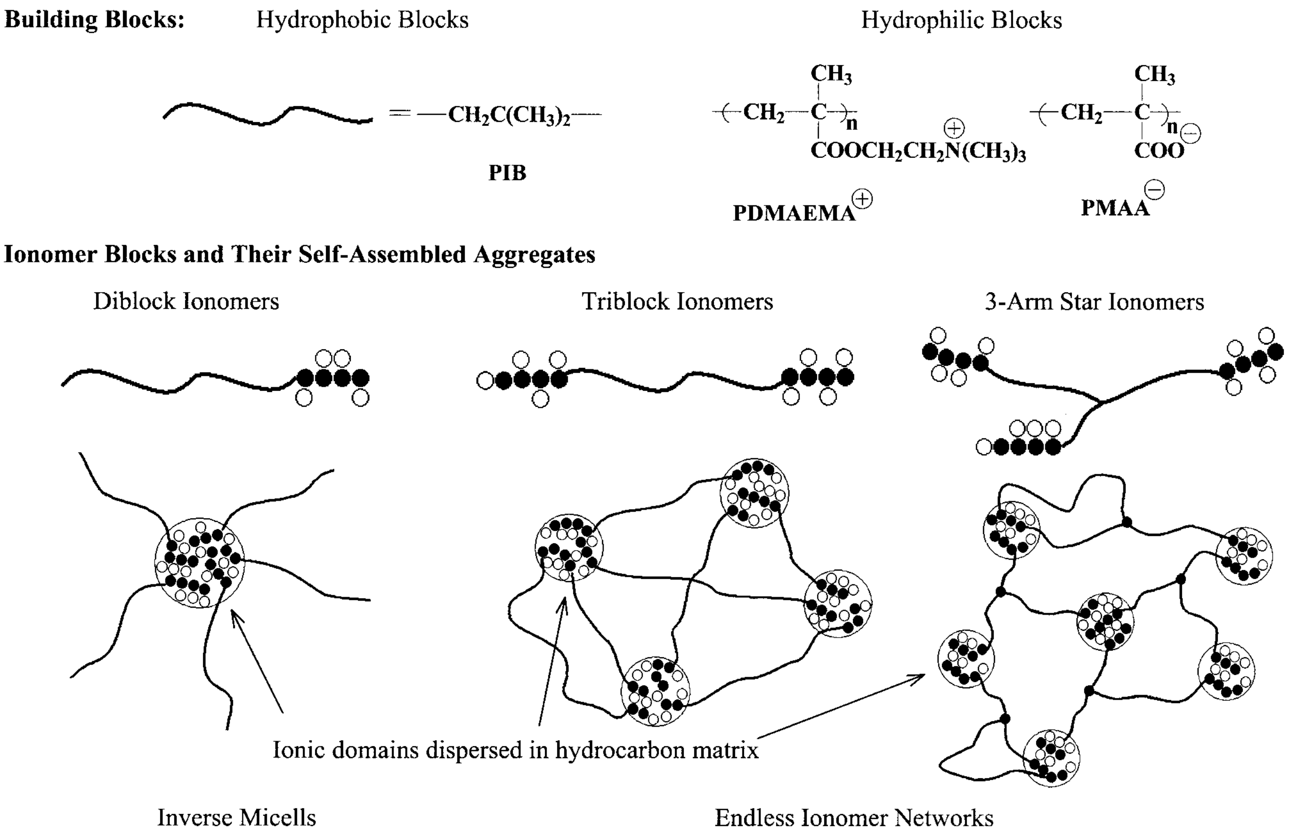

Scheme 1 Cationomers, anionomers, and their aggregates (reproduced from ref. 13). The open circle/closed circle symbolize ion/counterion pairs.

b-PMAA(7) stands for a triblock consisting of a PIB mid-block of DP = 160 flanked by two PMAA blocks of DP = 7.

Materials

Table I lists the materials used, together with their molecular characteristics. Neutralization of the PMAA blocks with zinc acetate [$Zn(AcO)_2$] or zinc strearate [$Zn(C_{17}H_{35}COO)_2$] led to anionomers, while quaternization of the PDMAEMA segments with CH_3I gave cationomers.[13,14] PIB and unionized ionomer precursors were used as controls.

Mechanical properties

The stress–strain relationship of block ionomers was studied by the use of ~1 mm thick samples cut by a microdumbell (ASTM D638, type 5) and an Instron 5567 instrument equipped with a video extensometer at room temperature. Samples were prepared by compression molding in a Carrer press between Teflon sheets at ~5,000 psi and slowly cooling to room temperature. Molding temperatures ranged from 150 to 250°C and depended on the specific sample. Samples were mounted with mechanical clamps 40 mm apart. The crosshead speed was 5 cm/min and a 50 kg load cell was used.

Rheological measurements

Dynamic mechanical analysis spectra were obtained by a dynamic mechanical spectrometer (ARES, Advanced Rheometric Expansion System). Ionomer samples for dynamic mechanical properties were prepared by molding ~200 mg of materials between 8 mm diameter parallel plates at a desired temperature for 30 min. Two pairs of parallel plates were used with 8 and 25 mm diameters. The 8 mm plates were for rigid samples, and the 25 mm plates were for viscous samples, such as PIB(3K). The gap between the plates was 0.5–1 mm. The spectrometer was equipped with a 200–2,000 g cm dual-range force rebalance transducer. Frequency dependences of G' and G'' were determined at select temperatures in the 30–300°C range. The time–temperature superposition was used whenever appropriate to obtain master curves. Liquid nitrogen was used to cool the samples. Temperature ramp measurements were carried out in the 30–300°C range at

TABLE I
Molecular Characteristics of Diblocks, Triblocks, and Three-Arm Star Precursors and Block Ionomers

Materials (numbers in parentheses indicate DP_n)	$M_{n,PIB}$ (g/mol)	$M_{n,PMAA}$ (g/mol)	$M_{n,PDMAEMA}$ (g/mol)	Polydispersity Index (M_w/M_n)
Diblocks				
PIB(54)	2,950			1.10
PIB(54)-*b*-POMAA(7)	2,950	540		1.31
PIB(54)-*b*-PDMAEMA(7)	2,950		1120	1.21
Blend of the latter two diblocks	2,950	540/1120		
Triblocks				
PIB(160)	8,770			1.23
PMAA(7)-*b*-PIB(160)-*b*-PMAA(7)	8,770	540		1.27
$PMAA^-$(7)-*b*-PIB(160)-*b*-$PMAA^-$(7), neutralized by $Zn(AcO)_2$	8,770	540		1.27
PDMAEMA(7)-*b*-PIB(160)-*b*-PDMAEMA(7)	8,770		1120	1.42
$PDMAEMA^+$(7)-*b*-PIB(160)-*b*-$PDMAEMA^+$(7), quaternized by CH_3I	8,770		1120	1.42
Blend of the two precursors	8,770	540/1120		
Three-arm stars				
$PIB(320)_3$	54,000			1.18
$\phi[PIB(320)\text{-}b\text{-}PMAA^-(4)]_3/Zn(AcO)_2$	54,000	300		1.24
$\phi[PIB(320)\text{-}b\text{-}PMAA^-(10)]_3/Zn(AcO)_2$	54,000	720		1.20
$\phi[PIB(320)\text{-}b\text{-}PMAA^-(18)]_3/Zn(AcO)_2$	54,000	1300		1.24
$\phi[PIB(320)\text{-}b\text{-}PMAA^-(10)]_3/Zn(C_{17}H_{35}COO)_2$	54,000	720		1.20

The syntheses of these materials were described in refs. 13 and 14.

1.0 rad/s oscillation frequency, 1% strain, and 2.0°C/min ramp rate.

RESULTS AND DISCUSSION

Steady-state shear flow

Investigations started by determining select viscoelastic properties of PIB. Figure 1 shows the steady-shear viscosity η and, for comparison, the absolute complex viscosity η^* of two linear and a three-arm star PIB as a function of shear rate.

Dynamic frequency sweep

Dynamic shear is typically employed for the study of viscoelastic characteristics. Figure 2 shows the G' and G'' master curves for PIB(54) and for the three-arm star $PIB(320)_3$. The data for sample PIB(160) are shown in Figure 3. These rheological data confirm earlier reported gel permeation chromatography results and also indicate that these materials are monodisperse.[13,14] The master curves forPIB(54) and PIB(160) do not intersect. The fact that the G' and G'' traces of PIB(54) and PIB(160) do not cross suggests that these ho-

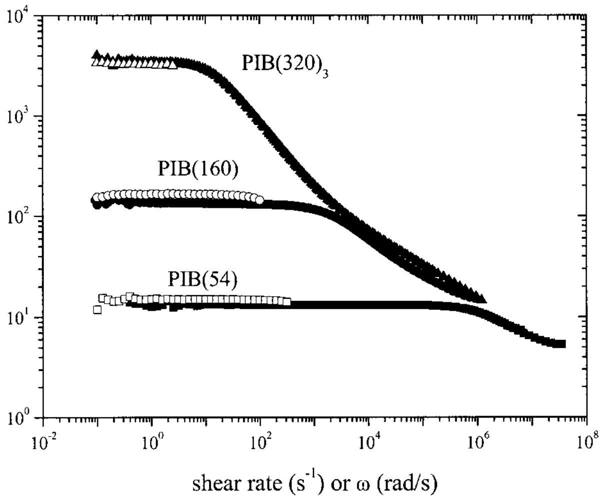

Figure 1 Steady-state shear viscosity at 40°C (η, open symbols) and master curves ([η^*], solid symbols) as a function of shear rate of various PIBs.

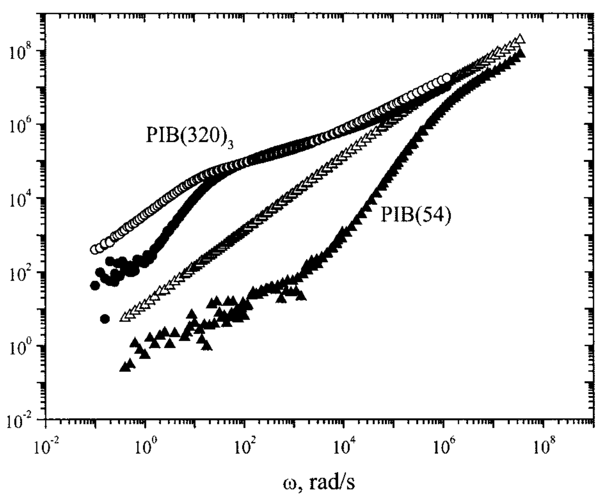

Figure 2 Comparison of master curves of G' (solid symbols) and G'' (open symbols) versus ω for a linear PIB and a three-arm star PIB. Reference temperature 40°C.

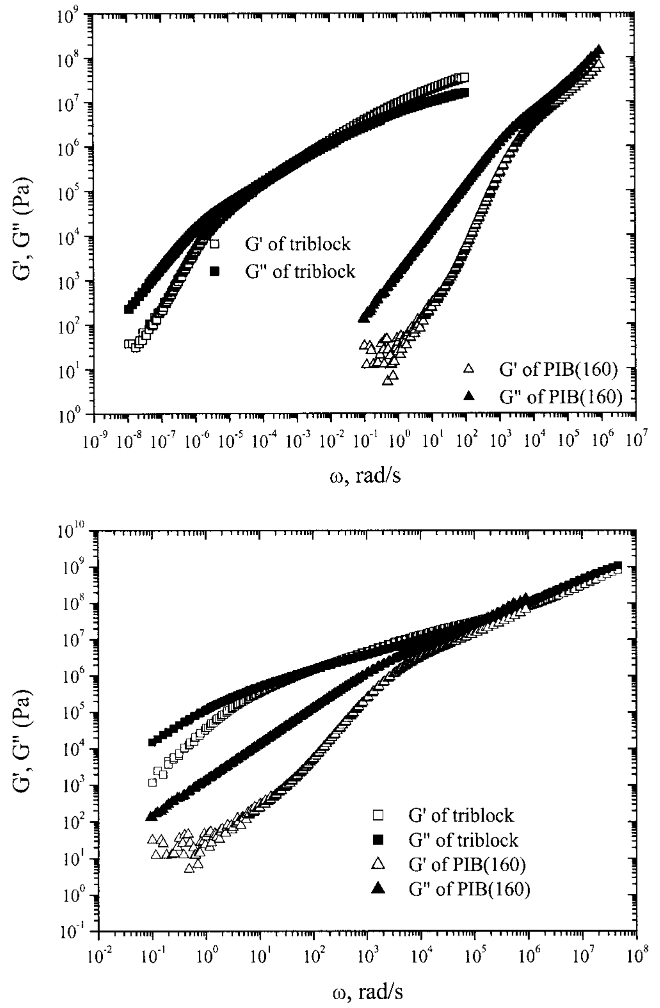

Figure 3 (a) Comparison of master curves of G' (open symbols) and G'' (solid symbols) versus ω for PIB(160) and PMAA(7)-PIB(160)-PMAA(7). Reference temperature 40°C. (b) Comparison of master curves of G' (open symbols) and G'' (solid symbols) versus ω for PIB(160) and PDMAEMA(7)-PIB(160)-PDMAEMA(7). Reference temperature 40°C.

mopolymers are below their entanglement molecular weights M_e (9,610 g mol^{-1}).[15] The G' and G'' traces of the three-arm star $\text{PIB}(320)_3$ are consistent with the characteristics of a star polymer.[16]

The viscoelastic properties of diblock copolymers PIB(54)-*b*-PMAA(7), PIB(54)-*b*-PDMAEMA(7), and their 50:50 (mol/mol) blend are rather different from those of the PIB homopolymers. The master curve of PIB(54)-*b*-PMAA(7) was taken at temperatures below 20°C using the time–temperature superposition [tTs; shown in Fig. 4(a)]. The data indicate micellization and that the packing of these micelles show solid-like mechanical behavior. The existence of the master curve suggests that the mesophase is thermally stable below 20°C. In contrast, as shown by the data in Figure 4(b), the material becomes unstable above ~40°C; its structure starts to vary with temperature

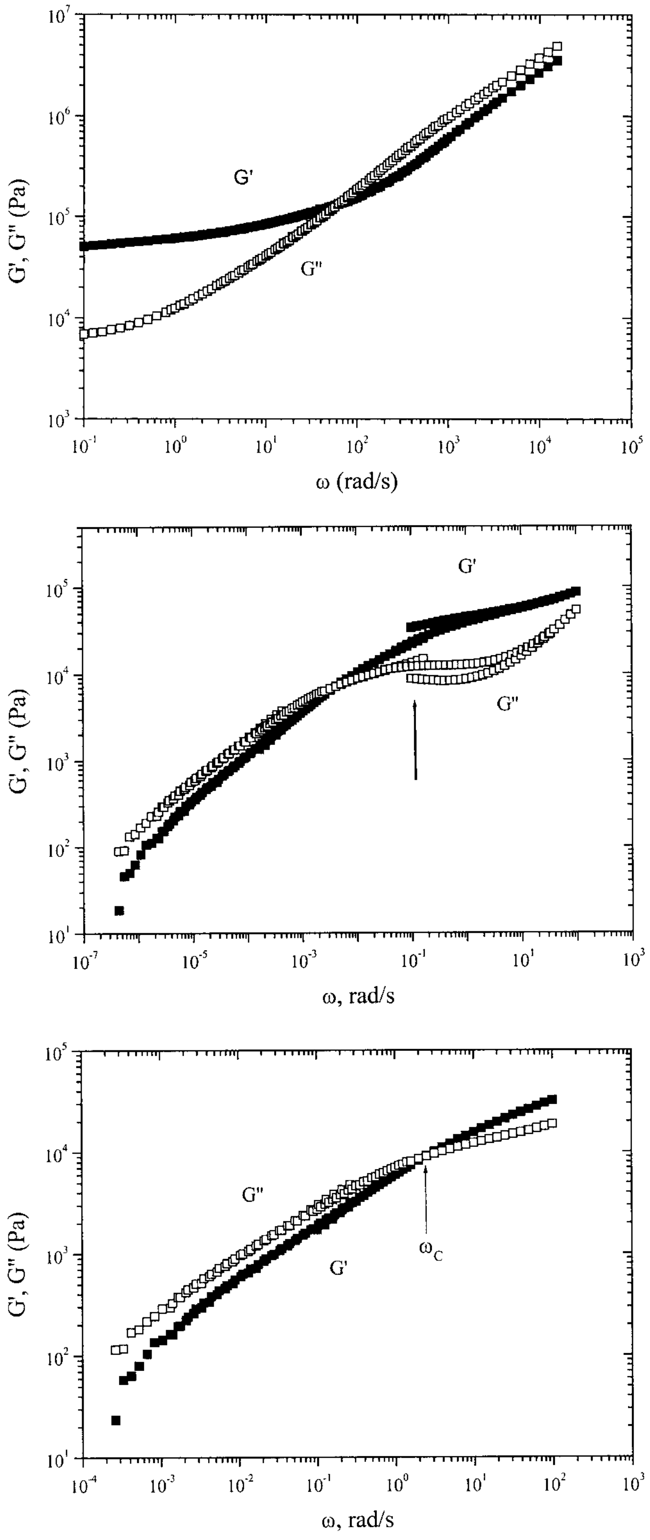

Figure 4 (a) Master curves of G' and G'' versus ω for PIB(54)-*b*-PMAA(7) below 20°C. Reference temperature 20°C. (b) Time–temperature superposition of G' and G'' versus ω for PIB(54)-*b*-PMAA(7) above 40°C. Reference temperature 40°C. The arrow indicates where the tTs breaks down. (c) Master curves of G' and G'' versus ω for PIB(54)-*b*-PMAA(7) above 80°C. Reference temperature 80°C. ω_c = crossover frequency.

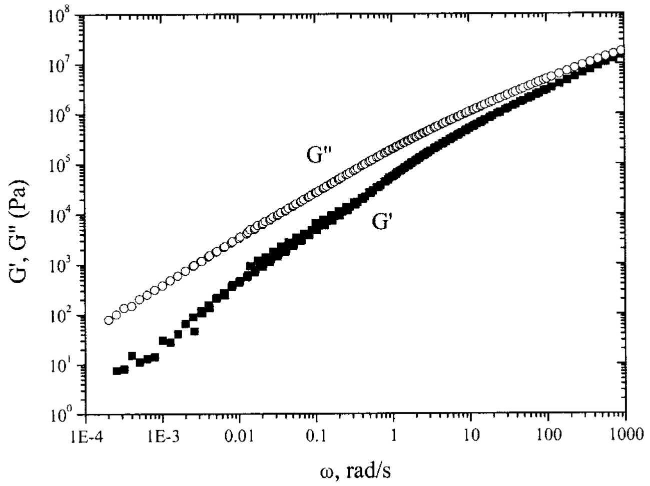

Figure 5 Master curves of G' and G'' versus ω for PIB(54)-*b*-PDMAEMA)(7). Reference temperature −30°C.

and the tTs breaks down. The structure becomes thermally stable again above 80°C, as shown by the data in Figure 4(c). Unlike PIB(54)-*b*-PMAA(7), PIB(54)-*b*-PDMAEMA(7) does not show solid-like viscoelastic behavior, as seen in Figure 5. The G' and G'' master curves for the 50:50 blend of these diblocks, shown in Figure 6, indicate a similar liquid-like viscoelastic behavior. All these samples exhibit a liquid-like region at sufficiently high temperatures.

PIB(54)-*b*-PMAA(7) is highly viscoelastic even at high temperatures. Hydrogen bonding between the carboxyl groups in the PMAA block most likely leads to the formation of micelles. The existence of hydrogen bonding in PIB-*b*-PMAA has been demonstrated by FTIR.[13] Hydrogen bonding prevails even above 80°C and leads to strong viscoelasticity, as shown in Figure 4(c). In contrast, PIB(54) is a viscous liquid that does not show interchain association at the same time scale. Apparently, PIB(54)-*b*-PDMAEMA(7) exhibits a much weaker interchain association. The blend of PIB(54)-*b*-PMAA(7) and PIB(54)-*b*-PDMAEMA(7) is also incapable of forming large structures and does not exhibit a crossover between G' and G''.

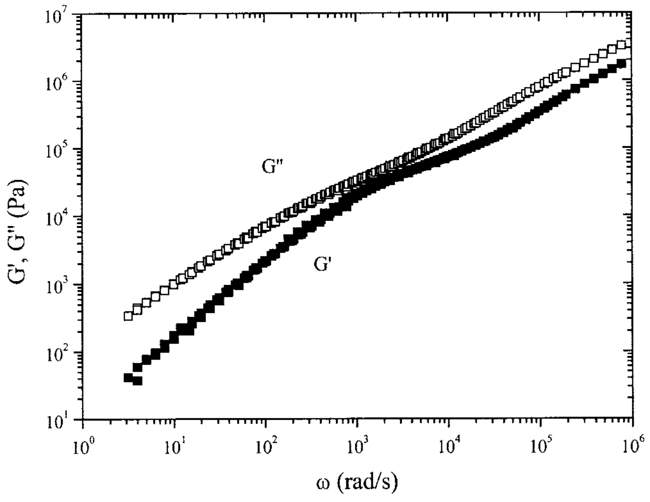

Figure 6 Master curves of G' and G'' versus ω for a 50:50 blend of PIB(54)-*b*-PMAA(7) and PIB(54)-*b*-PDMAEMA(7). Reference temperature 40°C.

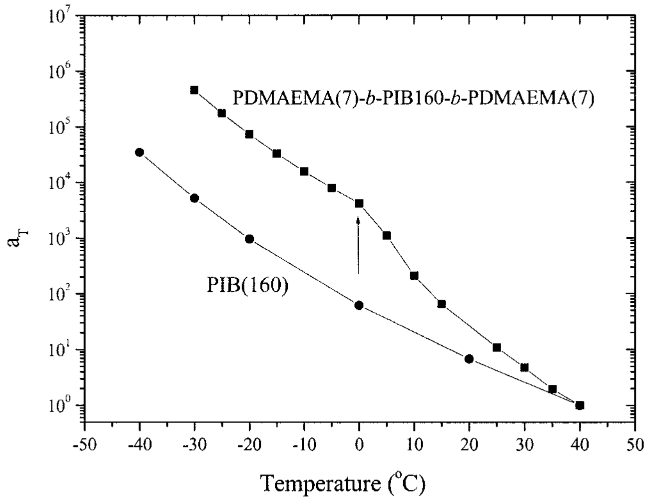

Figure 7 Temperature dependence of the shift factor a_T from −30°C to 40°C for PDMAEMA(7)-*b*-PIB(160)-*b*-PDMAEMA(7) and PIB(160). The arrow indicates the different temperature dependence of a_T for the two sequences in the triblock.

Triblocks PMAA(7)-*b*-PIB(160)-*b*-PMAA(7) and PDMAEMA(7)-*b*-PIB(160)-*b*-PDMAEMA(7) are, respectively, precursors for the anionomer PMAA$^-$(7)-*b*-PIB(160)-*b*-PMAA$^-$(7)/Zn^{++} and cationomer PDMAEMA$^+$(7)-*b*-PIB(160)-*b*-PDMAEMA$^+$(7)/I$^-$. Figure 3 shows the viscoelastic behavior of the precursors relative to that of PIB(160). Compared with the master curve for PIB(160), PMAA(7)-*b*-PIB(160)-*b*-PMAA(7) shows a dramatic change in both the shape and position of the crossover point. As shown in Figure 3, PIB(160) flows while the anionomer precursor is more elastic at 40°C. The master curve of PMAA(7)-*b*-PIB(160)-*b*-PMAA(7) exhibits behavior somewhat similar to that of a star polymer. The molecular weight of such a virtual star polymer is very high since it starts to show fluid-like behavior at $\omega = \sim 10^{-5}$ rad/s. It was also reported that one-arm end-functionalized zwitterionic can form supramolecular dendritic stars because of intermolecular associations.[11] In contrast, we cannot see such a dramatic difference between PDMAEMA(7)-*b*-PIB(160)-*b*-PDMAEMA(7) and PIB(160), as shown in Figure 3(b). This triblock copolymer exhibits a perfect master curve in the measured temperature range; however, the shift factor a_T shows two regions as shown in Figure 7.

As indicated by the data of PDMAEMA(7)-*b*-PIB(160)-*b*-PDMAEMA(7) in Figure 8(a), heating and

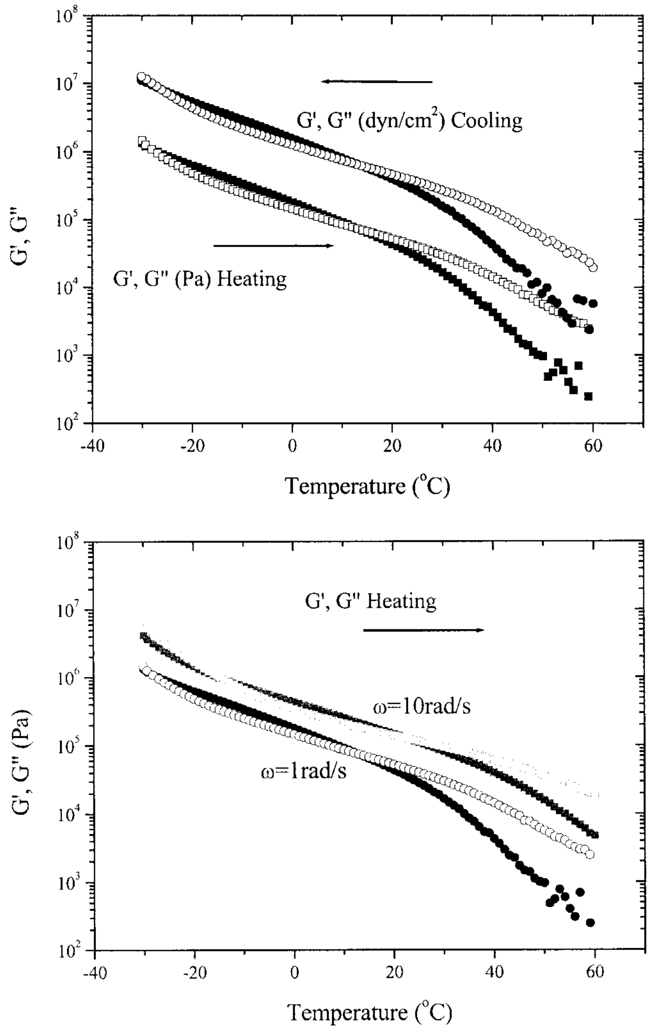

Figure 8 (a) Temperature dependences of the shift factor a_T from −30°C to 60°C, frequency 1 rad/s. (b) Temperature dependences of the shift factor a_T from −30°C to 60°C, frequency 10 rad/s

cooling yield almost identical curves for G' and G''. Similar curves arise when the probing frequency is changed from 1 to 10 rad/s (Fig. 8). The two groups of curves overlap perfectly by applying a horizontal shift; this indicates that the time–temperature superposition is satisfied.

The frequency dependences of G' and G'' at 40°C for the triblock anionomer PMAA$^-$(7)-*b*-PIB(160)-*b*-PMAA$^-$(7)/Zn^{++}, cationomer PDMAEMA$^+$(7)-*b*-PIB(160)-*b*-PDMAEMA$^+$(7)/I$^-$, and the 50:50 blend of these two ionomers are displayed in Figure 9(a–c), respectively. In all these cases, the materials are in rubbery region and this behavior prevails over a wide temperature range, indicating networks formation due to ionic associations. Figure 9(d) shows the frequency dependences of G' and G'' for the neutralized three-arm stars anionomers ϕ[PIB(320)-*b*-PMAA$^-$(10)]$_3$/Zn^{++} and ϕ[PIB(320)-*b*-PMAA$^-$(18)]$_3$/Zn^{++}. These data also indicate crosslinking.

The dynamic shear data clearly show that, due to ionic interactions, triblock anionomers based on PIB(160) exhibit rubbery behavior while diblock anionomers based on PIB(54) form micelles that exhibit elasticity at low temperatures and fluid-like behavior at high temperatures. It was also reported that neutralized polymers exhibit ionic crosslinks and consequently showed rubber-like viscoelasticity.[16]

Dynamic temperature ramp

Comparison of triblock anionomer, cationomer, and their blend

Figure 10(a–c) shows, respectively, the G' and G'' of triblock anionomer PMAA$^-$(7)-*b*-PIB(160)-*b*-PMAA$^-$(7)/Zn^{++}, cationomer PDMAEMA$^+$(7)-*b*-PIB(160)-*b*-PDMAEMA$^+$(7)/I$^-$, and the 50:50 during temperature ramp. The anionomer shows a sol-gel–type transition at 200°C, and the cationomer at 225°C. In both cases, the mechanical properties remain relatively unchanged below the softening ranges (or T_g) and show sharp transitions (melting) at these temperatures. At virtually identical segment molecular weights, the cationomer produces a weaker network than the anionomer. The relatively weak cationomer network is most likely due to the weak electrostatic forces prevailing between the large ammonium cation and iodine anion. These results correlate well with mechanical property data. The cationomer–anionomer blend shows a continuous decrease of G' and G'' with temperature. The blend retains its elastic characteristics even above 250°C, whereas the tribock anionomer collapses into a liquid at such temperatures.

These findings are in sharp contrast with those obtained with conventional thermoplastic elastomers and random ionomers that show much lower transition temperatures. These materials generally exhibit a continuous deterioration of mechanical properties with rising temperature due to relatively weaker interchain crosslinks.

Thermal stability

The thermal stability of the triblock anionomer has been studied. Figure 11 shows the results and summarizes the experimental procedure. The sample was heated to 175°C (A_1), cooled to ~40°C (A_2), heated to 200°C (B_1), cooled again (B_2), and finally heated to 250°C (C). Within experimental error, the material maintained its mechanical properties during both the heating and cooling circles. According to these observations, the network structure of the anionomer was maintained during repeated heating to elevated temperatures.

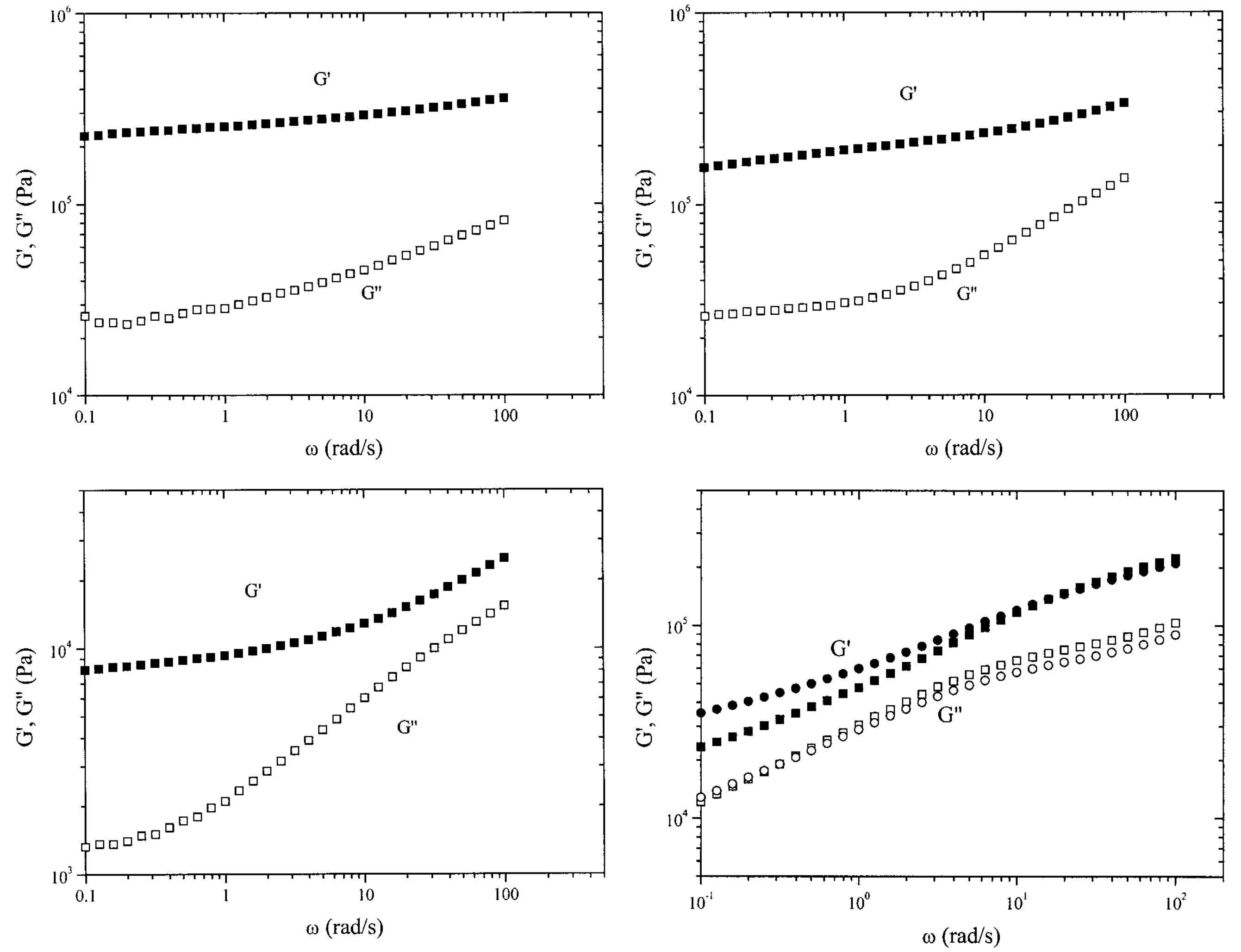

Figure 9 (a) Frequency sweep of PMAA$^-$(7)-*b*-PIB(160)-*b*-PMAA$^-$(7)/Zn^{++}, 40°C. (b) Frequency sweep of PDMAEMA$^+$(7)-*b*-PIB(160)-*b*-PDMAEMA$^+$(7)/I$^-$, 40°C. (c) Frequency sweep of PMAA$^-$(7)-*b*-PIB(160)-*b*-PMAA$^-$(7)/Zn^{++} and PDMAEMA$^+$(7)-*b*-PIB(160)-*b*-PDMAEMA$^+$(7)/I$^-$, 40°C. (d) Frequency sweeps of *ϕ*[PIB(320)-*b*-PMAA$^-$(n)]$_3$/Zn^{++}, n = 10 (squares) and n = 18 (circles), 40°C.

The effect of temperature on *G'* and *G"* of three-arm anionomers was studied. The experiments were carried out with two three-arm star anionomers, *ϕ*[PIB(320)-*b*-PMAA$^-$(4)]$_3$ and *ϕ*[PIB(320)-*b*-PMAA$^-$(10)]$_3$ neutralized with Zn(AcO)$_2$. Figure 12 shows the findings. Clearly, the longer ionic sequence produces a stronger and more stable network and exhibits a higher softening temperature. The processing temperature can be decreased by the use of zinc stearate [Zn($C_{17}H_{35}$COO)$_2$] instead of Zn(AcO)$_2$, because Zn($C_{17}H_{35}$COO)$_2$ functions both as a neutralizing agent and plasticizer.[17] In the case of *ϕ*[PIB(320)-*b*-PMAA$^-$(10)]$_3$, the softening points of the sample obtained by neutralization with Zn($C_{17}H_{35}$COO)$_2$ decreased to 220°C, compared with 260°C for the sample by using Zn(AcO)$_2$.

Sample *ϕ*[PIB(320)-*b*-PMAA$^-$(18)]$_3$ could not be compression-molded even by the use of Zn($C_{17}H_{35}$COO)$_2$. Thus, an effort was made to generate data by solution-coating a film of the precursor, *ϕ*[PIB(320)-*b*-PMAA$^-$(18)]$_3$, from THF solution containing a few drops of water and treating the film with a concentrated solution of Zn(AcO)$_2$. This technique, however, gave only a partially neutralized product with two transition temperatures: one at 200°C due to coulombic crosslinks by the carbonyl groups, and another at 350°C due to carbonyl groups sequences neutralized by Zn^{2+}. In contrast, we did not have this problem with the triblock anionomer [PMAA$^-$(7)-*b*-PIB(160)-*b*-PMAA$^-$(7)], and both techniques gave useful samples.

Mechanical properties

We were particularly interested in investigating the mechanical properties of triblock cationomers and anionomers. We knew that di- and tritelechelic PIB-based anionomers (i.e., linear and three-arm star PIBs

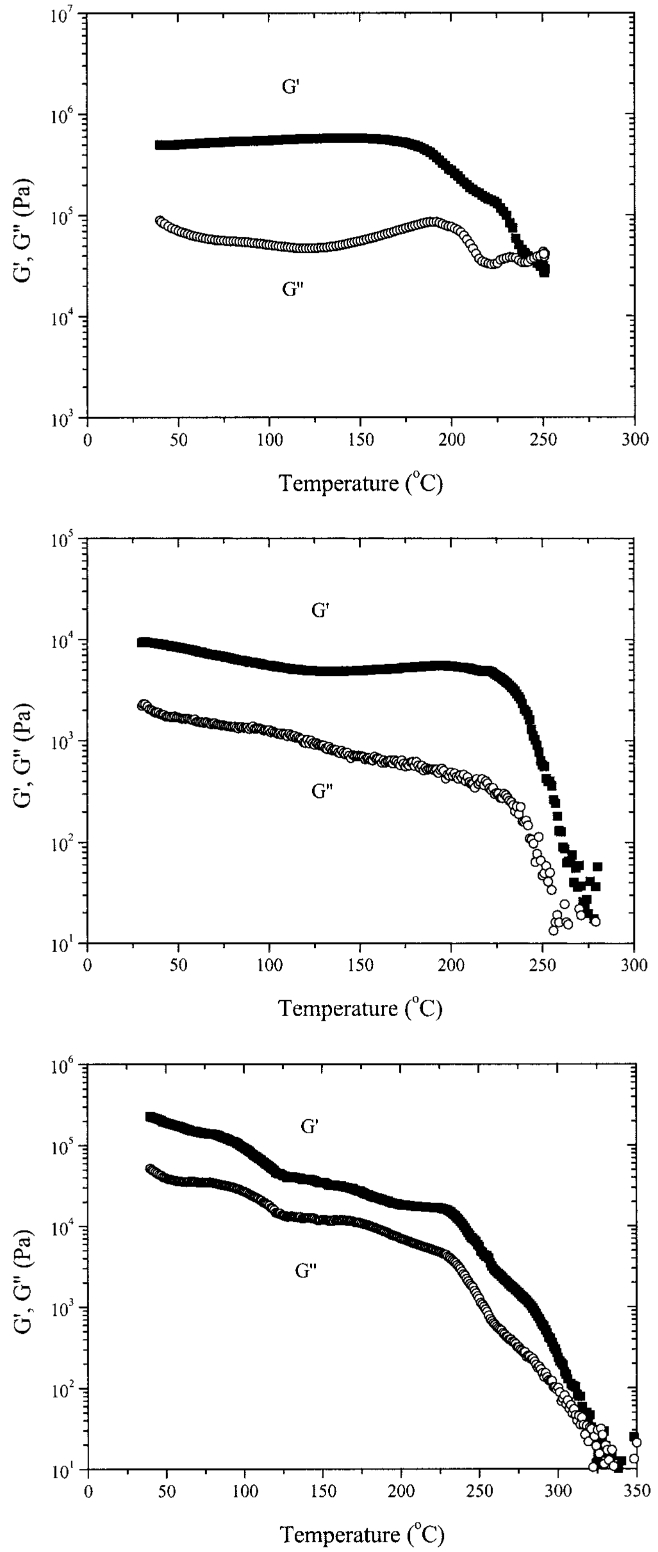

Figure 10 (a) The G' and G'' versus temperature of PMAA$^-$(7)-*b*-PIB(160)-*b*-PMAA$^-$(7)/Zn^{++}. (b) The G' and G'' versus temperature of PDMAEMA$^+$(7)-*b*-PIB(160)-*b*-PDMAEMA$^+$(7)/I$^-$. (c) G' and G'' versus temperature of triblock ionomer blend.

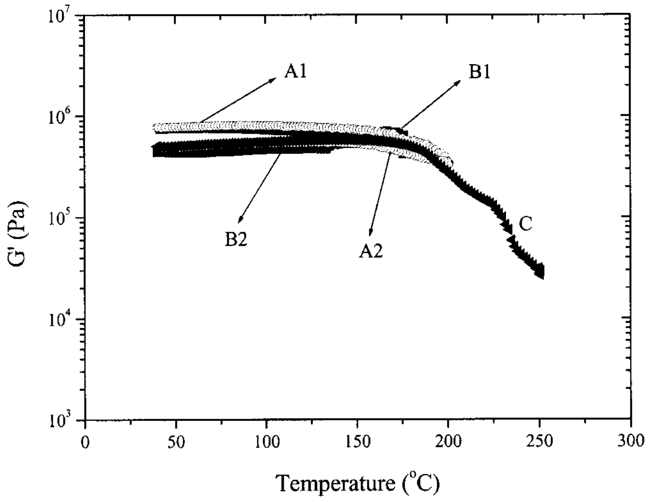

Figure 11 Testing of the reversibility over the heating–cooling durations using the triblock anionomer: A_1, 40°C to 175°C; A_2, 175°C to 40°C; B_1, 40°C to 200°C; B_2, 200°C to 40°C; C, 40°C to 250°C.

carrying a —$SO_3^+X^-$ group at the chain termini) are excellent thermoplastic elastomers (TPEs).[10] In view of the microstructure of our triblock and three-arm star block ionomers (Scheme 1), we expected self-assembly of the external ionic sequences attached to the internal rubbery PIB blocks and, consequently, the appearance of TPE characteristics.

Figure 13 shows stress–strain traces of PMAA$^-$(7)-*b*-PIB(160)-*b*-PMAA$^-$(7)/Zn^{++} and PDMAEMA$^+$(7)-*b*-PIB(160)-*b*-PDMAEMA$^+$(7)/I$^-$ and their blend. As anticipated, both the anionomer and the cationomer exhibited TPE characteristics. In view of the low molecular weight of the PIB segments, the strength and modulus of both block ionomers are remarkably high

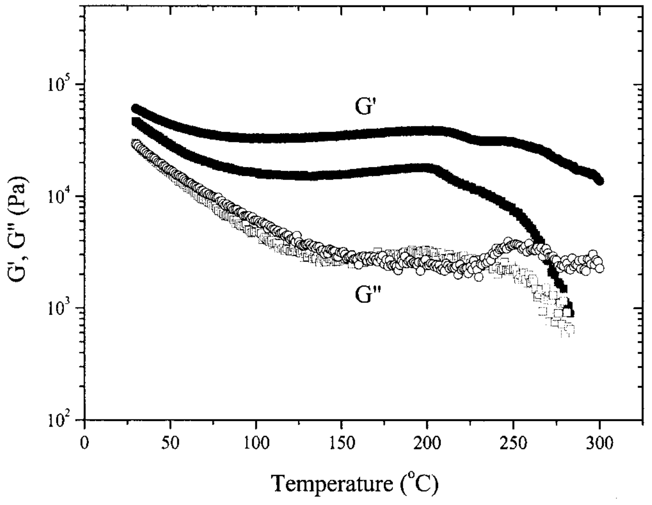

Figure 12 G' and G'' versus temperature of three-arm star anionomers: ϕ[PIB(320)-*b*-PMAA$^-$(4)]$_3$/Zn^{++} (squares), ϕ[PIB(320)-*b*-PMAA$^-$(10)]$_3$/Zn^{++} (circles).

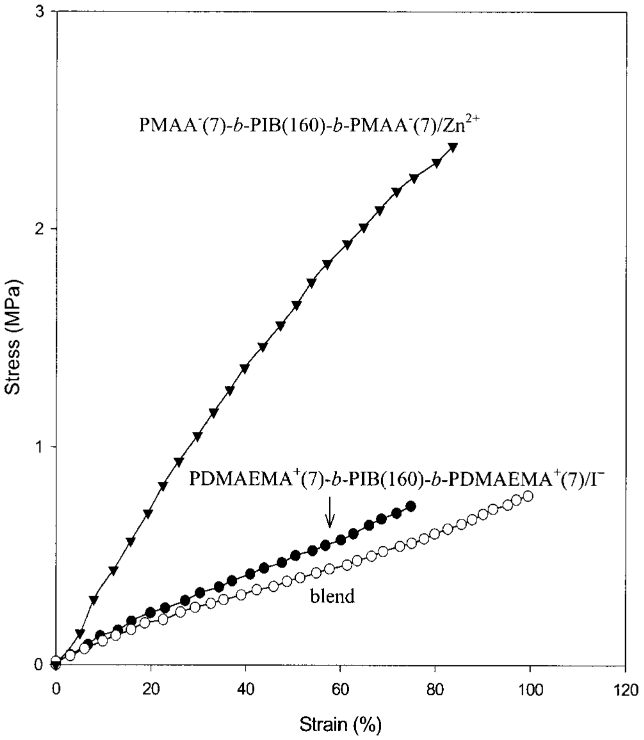

Figure 13 Stress–strain traces of anionomer $PMAA^{-}(7)$-*b*-PIB(160)-*b*-$PMAA^{-}(7)$, neutralized by $Zn(AcO)_2$, cationomer $PDMAEMA^{+}(7)$-*b*-PIB(160)-*b*-$PDMAEMA^{+}(7)$, quaternized by CH_3I, and their blend.

(PIB of DP = 160 is a viscous fluid). The length of the PIB blocks in these materials were kept low to avoid strength enhancement by entanglement. While the elongations of the two block ionomers were essentially the same (~80%) because of the same PIB block lengths, the anionomer showed far superior strength properties than the structurally very similar cationomer. One of the reasons for the low strength of the cationomer may be the relatively low ionic strength of the loose —$N^{+}(CH_3)_2/I^{-}$ ion pair. Evidently, the anionomer contains relatively smaller or tighter ion pairs (—$COO^{-}Zn^{++}$ ^{-}OCO—) and leads to more densely associated networks than the looser cationomer system. TPE properties would be expected to increase by using much higher molecular weight PIB and blocks with higher ionic strength (i.e., —$SO_3^{+}X^{-}$).

Figure 13 also shows the stress–strain traces of a cationomer–anionomer blend. The length of the PIB block and the number of ionizable groups in these block ionomers are identical. We postulate the formation of very large soft ion pairs by the —COOH groups in the PMAA segments protonating the —$N(CH_3)_2$ groups in the PDMAEMA blocks:

$$P\text{–}COOH + (CH_3)_2N\text{–}P \rightarrow P\text{–}COO^{-}\ H(CH_3)_2N^{+}\text{–}P$$

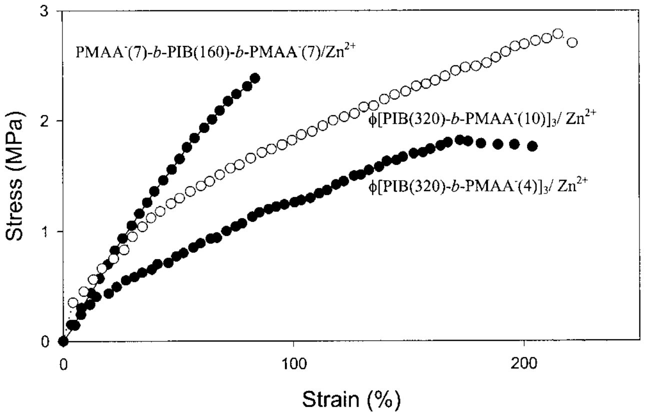

Figure 14 Effect of PIB block length and microarchitecture on the mechanical properties of select block ionomers.

The data shown in Figure 11 are in line with this expectation. While the elongation of the blend (~100%), which reflects the influence of the rubbery PIB block, is very similar to that obtained with either the anionomer or cationomer (~100% and ~80%), the modulus of the blend is even lower than that of the cationomer.

Figure 14 shows the tensile behavior of a triblock anionomer and two three-arm star block anionomers. Evidently, both the PIB block lengths and microarchitecture affect elongation. In regard to PIB block length, the elongation of the triblock, which contains one PIB block of DP_n = 160, is much shorter (~80%) than that of the three-arm stars (~210%), which contain three PIB blocks, each of DP_n = 320. The elongation of the two three-arm star block ionomers with the same-length PIB blocks are virtually identical (~210%).

The effect of zinc acetate and zinc stearate on the processing characteristics of EPDM-based ionomers has been studied by Lundberg and Makowski.[17] The addition of zinc stearate to sulfonated EPDM improved the melt flow and mechanical properties. We have compared the effect of zinc acetate and stearate on the mechanical properties of one of our three-arm

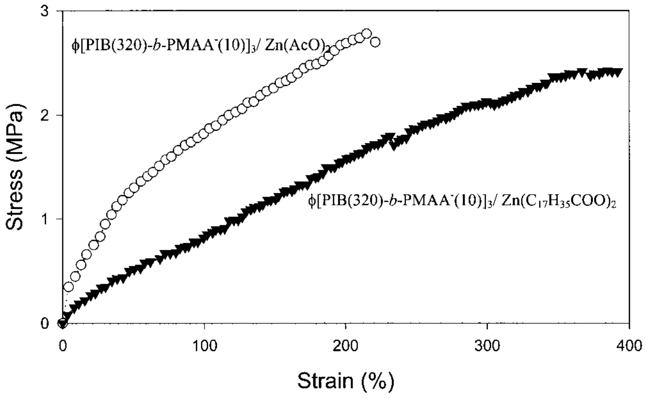

Figure 15 Comparison of the effect of zinc acetate and stearate on the mechanical properties of a three-arm star anionomer.

star block anionomers. Figure 15 contrasts the stress–strain characteristics of ϕ[PIB(18K)-*b*-PMAA^{-}(10)]$_3$ neutralized by $Zn(AcO)_2$ or $Zn(C_{17}H_{35}COO)_2$. The stearate (the larger counterion) leads to a more than doubling of elongation with very little if any deficit in strength. Evidently, the network is looser and softer in the presence of the larger stearate counterion.

CONCLUSIONS

The viscoelastic and mechanical properties of novel polyisobutylene-based block anionomers and cationomers, together with their precursors, were studied. Dynamic shear data of PIB(54)-*b*-PMAA(7) indicate inverse micelle formation. The product exhibits strong viscoelasticity, which suggests micelles packed into a solid-like arrangement. In the presence of large structures, the short chains would exhibit viscous liquid-like behavior at low frequencies and high temperatures. Hydrogen-bonding may account for the morphology. In contrast, PIB(54)-*b*-PDMAEMA(7) shows only weak viscoelasticity. PMAA(7)-*b*-PIB(160)-*b*-PMAA(7) exhibited impressively strong viscoelasticity, whereas PDMAEMA(7)-*b*-PIB(160)-*b*-PDMAEMA(7) was much weaker.

Neutralization of PMAA-*b*-PIB-*b*-PMAA and ϕ[PIB-*b*-PMAA]$_3$ with $Zn(AcO)_2$ or $Zn(C_{17}H_{35}COO)_2$, and quaternization of PDMAEMA-*b*-PIB-*b*-PDMAEMA with CH_3I produce anionomers and cationomers. The viscoelastic behavior and mechanical properties of the precursors change dramatically after their conversion to ionomers. Coulombic association between the ionic segments leads to physical crosslinks and give rise to rubbery materials with high transition temperatures. The mechanical properties of the ionic networks are stable below the transition temperature. The overall strengths of the ionic associations could be enhanced by increasing the length of the ionic segments.

References

1. Fredrickson, G. H.; Bates, F. S. Annu Rev Mater Sci 1996, 26, 501.
2. Bates, F. S.; Fredrickson, G. H. Annu Rev Phys Chem 1990, 41, 525.
3. Larson, R. G. The Structure and Rheology of Complex Fluids; Oxford University Press: New York, 1999.
4. Colby, R. H. Curr Op Colloid Interface Sci 1996, 1, 454.
5. Nguyen, D.; Kim, J.-S.; Guiver, M. D.; Eisenberg, A. J Polym Sci Polym Phys 1999, 37, 3226.
6. Moffitt, M.; Yu, Y.; Nguyen, D.; et al. J Polym Sci Polym Phys 1998, 31, 2190.
7. Yu, Y.; Zhang, L.; Eisenberg, A. Langmuir 1997, 13, 2578.
8. Yoshikawa, K.; Desjardins, A.; Dealy, J. M.; Eisenberg, A. Macromolecules 1996, 29, 1235.
9. Weiss, R. A.; Sen, A.; Pottick, L. A.; Willis, C. L. Polymer 1991, 32, 2785.
10. Storey, R. F.; Baugh, D. W. Polymer 2001, 42, 2321.
11. Vlassopoulos, D.; Pitsikalis, M.; Hadjichristidis, N. Macromolecules 2000, 33, 9740.
12. Vlassopoulos, D.; Pakula, T.; Fytas, G.; et al. J Chem Phys 1999, 111, 1760.
13. Fang, Z.; Kennedey, J. P. J Polym Sci Polym Chem 2002, 40, 3662.
14. Fang, Z.; Kennedey, J. P. J Polym Sci Polym Chem 2002, 40, 3679.
15. Tse, M. F.; Wang, H.-C.; Shaffer, T. D.; McElrath, K. O.; Krishnamoorti, R.; Modi, M. Presented at the Rubber Division, American Chemical Society Meeting, Cleveland, OH, October 21–24, 1997.
16. Eisenberg, A.; Kim, J.-S. Introduction to Ionomers; Wiley: New York, 1998.
17. Lundberg, R. D.; Makowski, H. S. J Polym Sci Polym Phys 1980, 18, 1821.